OsMADS6 Controls Flower Development by Activating Rice *FACTOR OF DNA METHYLATION LIKE1*[1][OPEN]

Juhong Tao,[a] Wanqi Liang,[a] Gynheung An,[b] and Dabing Zhang[a,b,c,2]

[a]Shanghai Jiao Tong University-University of Adelaide Joint Centre for Agriculture and Health, State Key Laboratory of Hybrid Rice, School of Life Sciences and Biotechnology, Shanghai Jiao Tong University, Shanghai 20040, China

[b]Crop Biotech Institute, Kyung Hee University, Youngin, Kyungbuk 446-701, Korea

[c]School of Agriculture, Food, and Wine, University of Adelaide, Waite Campus, Urrbrae SA 5064, Australia

ORCID IDs: 0000-0002-9965-552X (J.T.); 0000-0002-9938-5793 (W.L.); 0000-0002-8570-7587 (G.A.); 0000-0002-1764-2929 (D.Z.)

OsMADS6, an ancient *AGAMOUS-LIKE6* (*AGL6*)-like gene, has essential functions in specifying floral organ and meristem identity in rice (*Oryza sativa*). However, how *AGL6* genes control flower development remains largely unknown. In this study, we report that OsMADS6 directly targets *FACTOR OF DNA METHYLATION LIKE 1* (*OsFDML1*), a rice homolog of the *SUPPRESSOR OF GENE SILENCING3*-like gene *FACTOR OF DNA METHYLATION 1* (*FDM1*) from Arabidopsis (*Arabidopsis thaliana*). Arabidopsis *FDM1* is involved in RNA-directed DNA methylation and *OsFDML1* regulates flower development. The expression of *OsFDML1* overlaps with that of *OsMADS6* in the palea primordia and the ovule, and OsMADS6 directly promotes *OsFDML1* expression through binding to regions containing putative CArG motifs within the *OsFDML1* promoter during rice spikelet development. Consistent with the phenotypes of *osmads6* mutants, the *osfdml1* mutants showed floral defects, including altered palea identity with lemma-like shape containing no marginal region of palea, increased numbers of stigmas and fused carpels, and meristem indeterminacy. Moreover, transgenic plants overexpressing *OsFDML1* displayed floral defects, such as abnormal paleae. Phylogenetic analysis showed that *OsFDML1* homologs exist only in terrestrial plants. In addition, protein-protein interaction assays showed that OsFDML1 interacts with its close paralog OsFDML2, similar to the activity of OsFDML1 homologs in Arabidopsis. These results provide insight into how the ancient *AGL6* gene regulates floral development.

Angiosperms exhibit diverse flower morphologies, which are determined by the precise control of floral organ initiation and formation (Zhang et al., 2013). Previously, extensive molecular and genetic investigations in eudicot species, such as Arabidopsis (Arabidopsis thaliana) and *Antirrhinum majus*, led to the classical ABC model, in which A genes define the sepals, A and B genes together specify the petals, B and C genes together determine the stamens, C gene defines the pistils, and A and C genes seem to be antagonistic to each other (Coen and Meyerowitz, 1991). A-function genes (*APETALA1* [*AP1*], *AP2*, and *OVULATA*), B-function genes (*AP3*, *PISTILLATA*, *DEFICIENS*, and *GLOBOSA*), and C-function genes (*AGAMOUS* [*AG*] and *PLENA*) exhibit special expression patterns in Arabidopsis and *Antirrhinum* and are essential for flower development (Coen and Meyerowitz, 1991). The D-function gene *SEEDSTICK* specifies the ovule identity in Arabidopsis redundantly with *AG*, *SHATTERPROOF1* (*SHP1*) and *SHP2* (Pinyopich et al., 2003; Brambilla et al., 2007). Subsequently, a new class of MADS box genes, *SEPALLATA1/2/3/4* (*SEP1/2/3/4*), were described as E-function genes that specify the identity of all four floral whorls (Pelaz et al., 2000, 2001a,b; Ditta et al., 2004). With these findings, in addition to the ABC model, the "quartet model" was developed, which is directly linked to floral organ specification in different complex combinations of the five types of homeotic transcription factors, i.e. A, B, C, D, and E (Theissen and Saedler, 2001).

Distinct from all eudicots and other monocots, in grass (Poaceae) species, the spikelet constitutes the basic unit of the inflorescence (Barker et al., 2001; Kellogg, 2001; Rudall et al., 2005; Zhang and Yuan, 2014). Each rice (*Oryza sativa*) spikelet contains two rudimentary glumes, two sterile lemmas and a fertile floret consisting of one lemma and one palea in whorl 1, two lodicules in whorl 2, six stamens in whorl 3, and one pistil in whorl 4 (Bommert et al., 2005; Itoh et al., 2005; Whipple et al., 2007; Yuan et al., 2009; Kellogg, 2015; Zhang et al., 2017).

[1]This research was supported by the National Key Technologies Research and Development Program of China, Ministry of Science and Technology (grant nos. 2016YFD 0100804 and 2016YFE0101000); by the National Natural Science Foundation of China (31230051); by the H2020-MSCA-RISE-2015 project ExpoSEED (691109); by the Innovative Research Team, Ministry of Education; by the 111 Project (grant no. B14016); by the Australian Research Council (DP170103352); and by Australia-China Science and Research Fund Joint Research Centre grant ACSRF48187.

[2]Address correspondence to zhangdb@sjtu.edu.cn.

The author responsible for distribution of materials integral to the findings presented in this article in accordance with the policy described in the Instructions for Authors (www.plantphysiol.org) is: Dabing Zhang (zhangdb@sjtu.edu.cn).

D.Z., W.L., and G.A. designed the experiments; J.T. performed most of the experiments; J.T. and D.Z. wrote the article.

[OPEN]Articles can be viewed without a subscription.

www.plantphysiol.org/cgi/doi/10.1104/pp.18.00017

Recent research in some grass species, such as rice and maize (*Zea mays*), suggests a modified ABCDE model (Kyozuka et al., 2000; Nagasawa et al., 2003; Prasad et al., 2005; Chen et al., 2006; Dreni et al., 2007; Ohmori et al., 2009; Thompson et al., 2009; Gao et al., 2010; Kobayashi et al., 2010; Li et al., 2010, 2011; Wang et al., 2010; Duan et al., 2012; Sang et al., 2012). Investigation of the expression pattern and function of these homeotic transcription factors in grasses and core eudicots suggests that the ABC model is partially applicable in regulating flower development, even though they have functional divergence (Kyozuka et al., 2000; Preston and Kellogg, 2006; Prusinkiewicz et al., 2007; Ohmori et al., 2009; Reinheimer and Kellogg, 2009; Thompson and Hake, 2009; Zhang and Wilson, 2009; Li et al., 2011; Zhang et al., 2013; Zhang and Yuan, 2014). Briefly, the identities of whorl-1 organs in grasses are controversial, and the definition of A-function genes has not been well established yet.

The function of B genes seems highly conserved in both monocots and eudicots based on the finding of homeotic mutations of *Silky1* in maize and *SUPERWOMAN1* (*SPW1*) in rice, orthologous to the B gene *AP3* in Arabidopsis. These mutations transform the lodicule and stamen into lemma/palea-like and carpel organs, respectively (Ambrose et al., 2000; Nagasawa et al., 2003; Whipple et al., 2007). The double mutants of two rice C genes, *OsMADS3* and *OsMADS58*, display the conversion of carpel into a palea-like structure, suggesting that *OsMADS3* and *OsMADS58* redundantly regulate stamen and carpel identity and flower meristem determination, mimicking the function of the ortholog *AG* in Arabidopsis (Dreni et al., 2011). This clearly indicates that C function is conserved within flowering plants (Dreni et al., 2011; Dreni and Kater, 2014). Rice contains two D function genes, namely, *OsMADS13* and *OsMADS21* (Dreni et al., 2007; Li et al., 2011), and *OsMADS13* specifies ovule identity and floral meristem determination, together with *OsMADS3* and *OsMADS58* (Dreni et al., 2011; Hu et al., 2015). Although *OsMADS21* does not seem to be crucial for reproductive organ formation, its protein product retains the potential of ovule identity specification (Dreni et al., 2011).

Rice possesses at least five *SEP*-like genes, namely, *OsMADS1/LEAFY HULL STERILE1* (*LHS1*), *OsMADS5*, *OsMADS7*, *OsMADS8*, and *OsMADS34/PANICLE PHYTOMER2*, and they have divergent functions during flower development (Malcomber and Kellogg, 2004, 2005; Zahn et al., 2005; Arora et al., 2007; Wu et al., 2018). *OsMADS1* specifies the floral organ identity and meristem determination (Jeon et al., 2000; Agrawal et al., 2005; Prasad et al., 2005; Chen et al., 2006; Hu et al., 2015). Transgenic plants in which the expression of *OsMADS1*, *OsMADS5*, *OsMADS7*, and *OsMADS8* is simultaneously reduced show homeotic conversion of all floral organs, except the lemma, into leaf-like structures, mimicking the defects observed in *sep1 sep2 sep3 sep4* quadruple mutants in Arabidopsis (Cui et al., 2010). *OsMADS34* plays critical roles in rice inflorescence and spikelet development (Gao et al., 2010; Kobayashi et al., 2010). *OsMADS32/CHIMERIC FLORAL ORGANS1* is a rice-specific MADS gene with critical roles in specifying floral organ identity by interacting with *OsMADS2* and *OsMADS4* (Sang et al., 2012; Wang et al., 2015).

AGL6 genes are ancient, found in both gymnosperms and angiosperms, and they are closely related to *SEP*- and *AP1*-like genes at the sequence level (Reinheimer and Kellogg, 2009; Li et al., 2010; Dreni and Zhang, 2016; Callens et al., 2018). Recent studies from monocots and core eudicots indicate that *AGL6*-like genes function in flower development (Reinheimer and Kellogg, 2009; Li et al., 2010; Dreni and Zhang, 2016). In grasses, *AGL6*-like genes have the ancient expression pattern in the ovule, but a diversified pattern in the palea (Reinheimer and Kellogg, 2009; Dreni and Zhang, 2016). Rice contains two *AGL6*-like genes: *OsMADS17* plays minor and redundant roles, whereas *OsMADS6* is a key regulator of flower development (Ohmori et al., 2009; Dreni and Zhang, 2016). *OsMADS6* regulates flower development of four whorls in rice, similar to the function of *SEP* in Arabidopsis (Ohmori et al., 2009; Li et al., 2010; Dreni and Zhang, 2016). Allelic mutants of *OsMADS6* exhibit obvious defects in floral organ identity specification and meristem determination, showing wider lemma-like palea (Ohmori et al., 2009; Li et al., 2010; Zhang et al., 2010; Duan et al., 2012). In addition, their lodicules and stamens homeotically exhibit conversion into glume-like or mosaic structures, and ectopic carpels develop occasionally (Ohmori et al., 2009; Li et al., 2010; Zhang et al., 2010; Duan et al., 2012). Moreover, *OsMADS6* genetically interacts with other B, C, D, and E MADS genes in specifying floral organ identity and meristem fate during spikelet development (Li et al., 2010, 2011). OsMADS6 forms a protein complex with OsMADS1 (Moon et al., 1999), and *osmads6 osmads1* (*mfo1-2 lhs1-2*; *osmads1-z osmads6-1*) display severe defects of floral meristem identity, which suggests that OsMADS6 and OsMADS1 together specify the state of rice flowers (Ohmori et al., 2009; Li et al., 2010). The specification of floral organ identity of the inner three whorls and meristem fate strongly depends on the additive effects and redundant functions of *OsMADS6* with *OsMADS16*, *OsMADS3*, and *OsMADS13* (Li et al., 2011). Interestingly, OsMADS6 may directly activate *OsMADS58* by binding to a putative CArG box motif, and the double mutant *osmads6-1 osmads58* exhibits higher numbers of stigmas and ectopic carpels/ovules, although it dramatically exhibits the phenotype of *osmads6-1* in the outer three whorls (Li et al., 2011). These reports suggest that autoregulation exists between these MADS box genes. Undoubtedly, *OsMADS6* plays key roles in rice spikelet specification by interacting with other homeotic MADS box genes. Thus, as an indispensable homeotic transcription factor in rice spikelet establishment, an underlying regulating network of *OsMADS6* is expected.

In this study, we report that OsMADS6 directly activates the expression of one target gene *OsFDML1*, which is homologous to *SUPPRESSOR OF GENE SILENCING3* (*SGS3*)-like genes in Arabidopsis. *OsFDML1* belongs to the gene family found only in terrestrial plants and mainly expressed in inflorescence and spikelet organs. Mutants of *OsFDML1* and ectopic expression of *OsFDML1* caused abnormal flower development. This work defines a regulatory pathway of *AGL6*-like genes in regulating flower morphogenesis.

RESULTS

OsFDML1 Is a Direct Target of OsMADS6

To clarify the regulatory role of OsMADS6, we performed additional analyses from the microarray data of the *osmads6-1* mutant at spikelet developmental stage Sp6 generated by Li et al. (2011). From the genes with changed expression in *osmads6-1* (Li et al., 2011), we selected eight genes encoding transcription factors and kinases for further study (Supplemental Table S1). Reverse transcription quantitative PCR (RT-qPCR) analysis using 2- to 3-mm-long young inflorescences at stages of spikelet development Sp6 confirmed that seven genes were upregulated and one gene was downregulated in *osmads6-1*.

To test whether OsMADS6 directly regulates the expression of these eight genes, we cloned the coding sequence of *OsMADS6* into the hormone-inducible expression vector LexA-VP16-ER (XVE), which employs the human estrogen receptor (hER) to confer β-estradiol inducible expression of a chimeric transcription factor (Zuo et al., 2006). Using the 0.5- to 1-cm root tips from 1-week-old young seedlings of transgenic plants containing *OsMADS6* fused with XVE (henceforth referred to as InDE6), we observed that the expression of LOC_Os02g19130, encoding a putative transcription factor X1 gene, was rapidly increased after 12 h of treatment with 5 μmol/L β-estradiol (Fig. 1B). The expression level was similar to that of the expression of *OsMADS6* in transgenic plants of InDE6 (Fig. 1B).

Based on the decreased expression of this gene in *osmads6-1* at stages Sp4, Sp6, and Sp8 during spikelet development (Fig. 1A), we expected that this gene (LOC_Os02g19130) would probably be a direct target of *OsMADS6*. Since LOC_Os02g19130 is homologous to the *SGS3*-like gene *FACTOR OF DNA METHYLATION1/2/3/4/5* (*FDM1/2/3/4/5*) in Arabidopsis, we renamed it rice *FACTOR OF DNA METHYLATION LIKE 1* (*OsFDML1*).

We then performed chromatin immunoprecipitation (ChIP)-qPCR analysis using 2- to 8-mm-long young inflorescences and purified rabbit polyclonal antibodies against OsMADS6 (Li et al., 2011). ChIP-qPCR showed specific enrichment of the 198-bp DNA fragment containing the putative CArG motif M1 (CCTATATTTG) within the *OsFDML1* promoter, but not the 200-bp DNA fragment containing the unclassical CArG motif M2 (CAAATTAAG) close by to the motif M1 (Fig. 1, C and D). In addition, yeast one-hybrid results showed that OsMADS6 could bind to the fragment containing the putative CArG motif and activate the expression of the *HIS3* nutritional reporter gene in the vector (Fig. 1E). Furthermore, compared with the empty vector and the modified one containing the tag Flag as negative controls, only the fused protein of OsMADS6-Flag triggered significantly increased expression of *OsFDML1pro:LUC* by coexpressing *OsFDML1pro:LUC* transiently with OsMADS6-Flag in *Nicotiana benthamiana* leaves (Fig. 1F). Taking these results together, we propose that OsMADS6 directly activates the expression of *OsFDML1* by binding to the regions containing the putative CArG motif within the *OsFDML1* promoter during rice spikelet development.

Expression and Phylogenetic Analysis of *OsFDML1*

To address the function of *OsFDML1*, we performed RT-qPCR and showed that the expression of *OsFDML1* mainly occurred in the spikelet and was strong in pistils but very weak in roots, stems, and leaves (Fig. 2A). In addition, our mRNA in situ hybridization results showed signals of *OsFDML1* transcripts mainly at the tip of the palea in longitudinal sections (Fig. 2, B–D), and these signals disappeared very soon after the initiation of stamens (inflorescence length 4–7 mm; Fig. 2E). Furthermore, expression of *OsFDML1* was seen in lemma primordia only at stage Sp2 (inflorescence length 1–1.5 mm; Fig. 2B). Surprisingly, we detected expression of *OsFDML1* specifically in the stamen adjacent to the palea, but not in other stamens (Fig. 2, D and E). Moreover, expression of *OsFDML1* was detected during the initiation of the carpel and ovule (Fig. 2, E and F). We detected *OsFDML1* RNA signals in the nucellus and strong signals in the ovule, but relatively weak signals in the integument of the ovary (Fig. 2, G and H). The strongest signals were detected in 5-d-old young embryo and vascular bundle (Fig. 2, I, J, and L). With nucellus maturation, we detected relatively weak expression of *OsFDML1* in the inner layer of the pericarp, young endosperm, and aleurone layer (Fig. 2, I and K), and no transcripts in the 10-d-old ovary (Fig. 2M). Moreover, expression of *OsFDML1* was almost undetectable in *osmads6-1* floral organs on mRNA in situ hybridization (Fig. 2, N–R), which is consistent with the regulatory role of OsMADS6 in activating the expression of *OsFDML1*. Overall, the expression of *OsFDML1* mostly overlapped that of *OsMADS6* in the floral organs, confirming that OsMADS6 is critical in modulating the expression of *OsFDML1* during flower development.

To determine the evolutionary relationship of *OsFDML1*-like genes, we used the full-length protein sequence of *OsFDML1* as a query to search the homologs of OsFDML1 in the proteome database (http://phytozome.jgi.doe.gov) and Congenie database (http://congenie.org). In total, we obtained 119 *OsFDML1*-like genes from 14 terrestrial plant species, including *Physcomitrella patens*, gymnosperms,

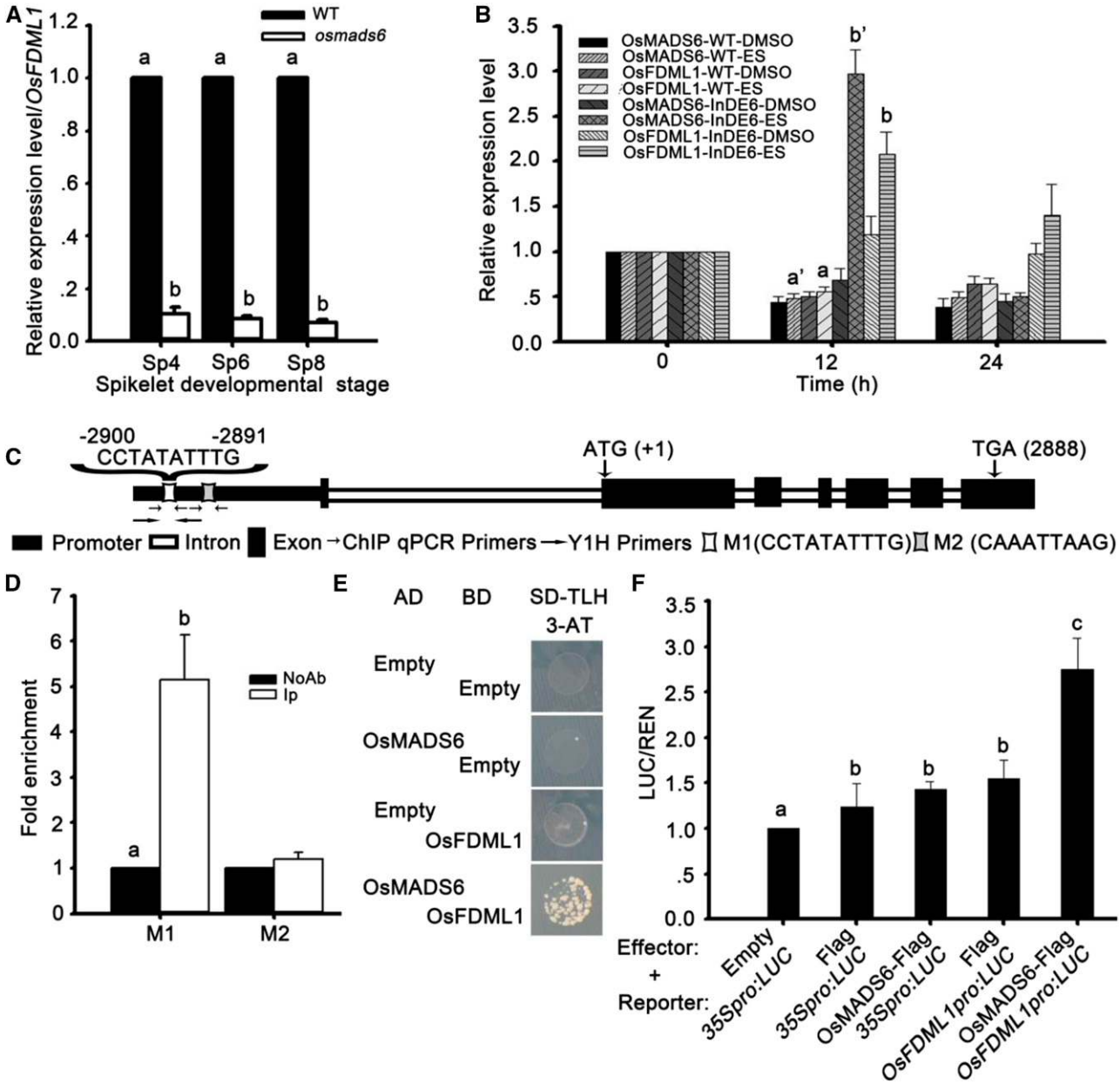

Figure 1. OsMADS6 directly activates the expression of *OsFDML1* in vivo during rice spikelet development. A, The expression of *OsFDML1* decreased in *osmads6-1* at spikelet developmental stages Sp4, Sp6, and Sp8. Spikelets at stages Sp4, Sp6, and Sp8 were collected from inflorescences of lengths 2, 2 to 3, and 4 to 7 mm, respectively. B, The expression of *OsFDML1* increased with the induced expression of *OsMADS6* in the transgenic plants InDE6. C, Diagram of *OsFDML1* gene with promoter regions containing the putative CArG motif. D, ChIP-qPCR results showed OsMADS6 can directly bind to *OsFDML1* promoter regions with putative CArG motif (M1) using 2- to 8-mm-long young inflorescences. The mock treatment included negative control treated without antibody and 200-bp *OsFDML1* promoter region containing an unclassical CArG motif M2 close by to the motif M1. The fold enrichment was calculated relative to the negative control without antibody. E, OsMADS6 bound to the *OsFDML1* promoter regions with putative CArG motif (M1) and activated the expression of nutritional reporter gene *HIS3* by yeast one-hybrid assay. F, OsMADS6 triggered the expression of *OsFDML1pro:LUC* with integrating 3795-bp *OsFDML1* genome sequence upstream of the ATG before LUC. All data are means ± SD ($n \geq 3$). Letters a, b, c, a′, and b′ represent statistical significance, $P < 0.05$. IP, Immunoprecipitation with specific antibody against OsMADS6; InDE6, transgenic plants containing *OsMADS6* fused with XVE; ES, β-estradiol.

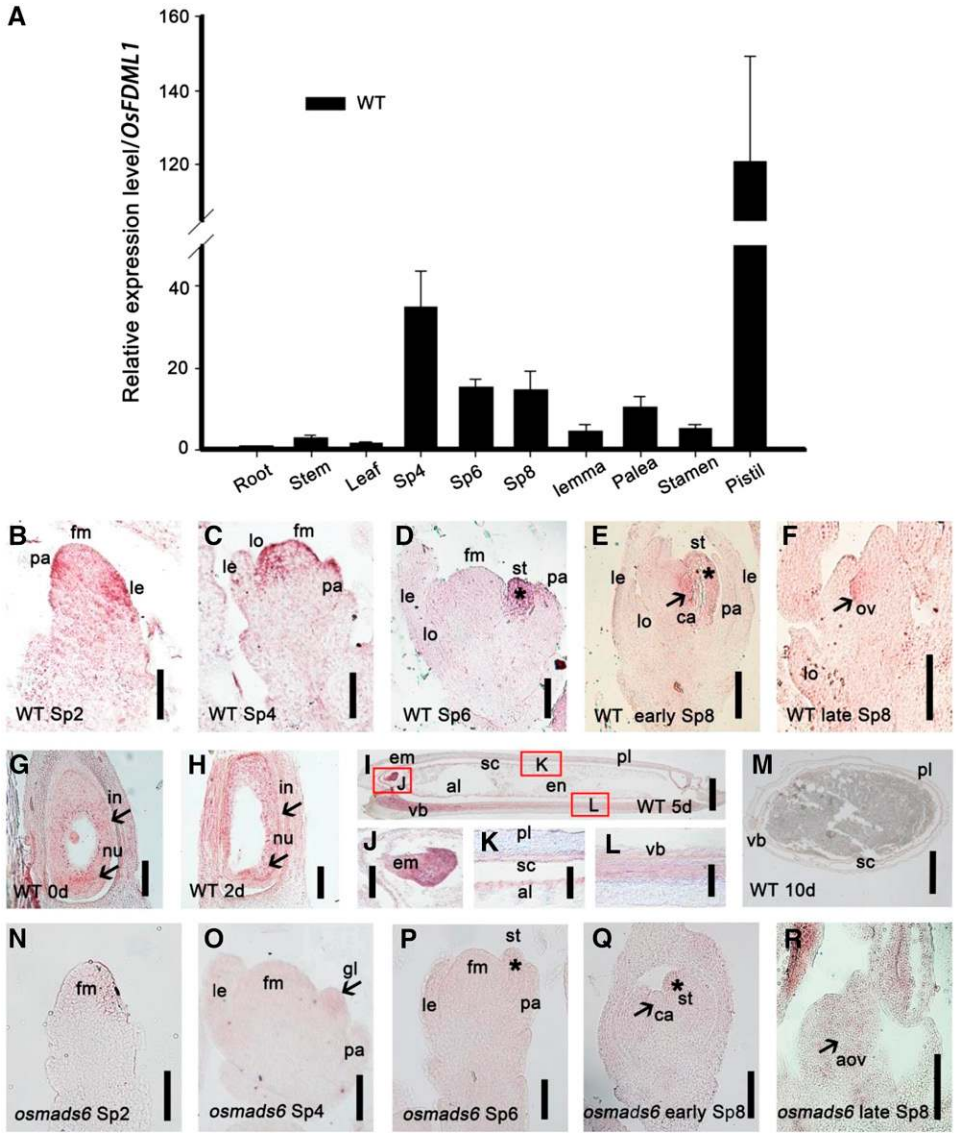

Figure 2. Expression pattern of *OsFDML1* in the wild-type and *osmads6-1* young spikelets. A, RT-qPCR analysis of the expression of *OsFDML1* in wild-type root, stem, leaf, and spikelets at stages Sp4, Sp6, and early Sp8, and dissected lemma, palea, stamen, and pistil, respectively. Root was collected from young seedlings cultivated 10 d in water. Stem and leaf were collected when the plants changed to reproductive growth phase. Spikelets at stages Sp4, Sp6, and Sp8 were sampled from inflorescences of lengths ~2, 2 to 3, and 4 to 7 mm, respectively. Lemma, palea, stamen, and pistil were dissected from the spikelets of length ~6 mm. All data are means ± SD ($n \geq 3$). B to F, In situ hybridization experiment showing the expression of *OsFDML1* in wild-type young spikelets at stages Sp2, Sp4, Sp6, early Sp8, and late Sp8. Spikelets at stages Sp2, Sp4, Sp6, early Sp8, and late Sp8 were sampled from inflorescences of lengths ~1 to 1.5, 2, 2 to 3, 4 to 7, and 10 to 20 mm, respectively. Asterisks indicate the palea side stamen in D and E. Arrowheads indicate the carpel primordia in E and the ovule in F. G to M, In situ hybridization experiment showing the expression of *OsFDML1* in wild-type ovaries representing 0, 2, 5, and 10 d since pollination. J to L, partial enlargements of I. Arrowheads indicate the integument and nucellus in G and H, respectively. Red rectangles indicate the position of J to L in I. N to R, In situ hybridization experiment showing the expression of *OsFDML1* in *osmads6-1* spikelets at stages Sp2, Sp4, Sp6, early Sp8, and late Sp8, respectively. Asterisks indicate the palea side stamens in P and Q. Arrowheads indicate the glume-like structure of *osmads6-1* in O, carpel primordia of *osmads6-1* in Q, and the abnormal ovule of *osmads6-1* in R. le, Lemma; pa, palea; gl, glume-like structure; lo, lodicules; st, stamen; fm, floral meristem; ca, carpel; ov, ovule; aov, abnormal ovule; nu, nucellus; in, integument; em, embryo; pl, pericarp; sc, seed capsule; al, aleurone; vb, vascular bundle. Bars = 50 μm in B, C, F, N, O, and R, 100 μm in D, E, J to L, P, and Q, and 500 μm in G to I and M.

monocots, and core eudicots, but no close relatives in green algae (Supplemental Table S2). In addition, most of the *OsFDML1*-like members contained the conserved XS (named after rice homolog X and Arabidopsis SGS3) and XH (rice gene X Homology) domains (Bateman, 2002), presented as tandem repeats with dramatic sequence variation. Therefore, phylogenetic analysis using the mostly conserved XH domain from *P. patens* moss; *Pinus taeda* (a gymnosperm); *Amborella trichopoda* (a sister species to all the extant angiosperms); Arabidopsis, *Prunus persica*, and *Vitis vinifera Genoscope* (core eudicots); rice and *Brachypodium distachyon* (commelinid monocots, Poaceae); and *Ananas comosus* and *Musa acuminata* (other commelinid monocots) from both the maximum likelihood and neighbor-joining approaches failed to obtain highly supported nodes. However, our sequence analysis suggested that these *OsFDML1*-like genes might have specific functions in terrestrial plants and undergo frequent tandem duplications and sequence variation as well as functional diversification. Further studies on the molecular mechanisms and generation of more knockout or knockdown mutants will clarify the global functions of this gene family.

The *osfdml1* Mutants Exhibit Defects in Floral Organ Identity and Meristem Determination

To further clarify the function of *OsFDML1*, we identified two *osfdml1* mutants: *osfdml1-1* (PFG_1C-03064, Korea) containing a T-DNA inserted at the N terminus of the first exon, and *osfdml1-2* (NE4801, Japan) containing a *Tos17* retrotransposon inserted at the C terminus of the first exon (Supplemental Fig. S1A). RT-PCR results using mRNA extracted from the 0.5-cm-long inflorescence at spikelet developmental stage Sp8 revealed that expression of *OsFDML1* was almost undetectable in *osfdml1-1* (Supplemental Fig. S1B). The expression of *OsFDML1* after *Tos17* insertion was significantly reduced in *osfdml1-2*, whereas the transcript level of *OsFDML1* before *Tos17* insertion showed no significant change (Supplemental Fig. S1B). Moreover, RT-qPCR showed that the expression of *OsFDML1* after *Tos17* insertion was reduced to approximately half of that in *osfdml1-2* (Supplemental Fig. S1C). Therefore, *osfdml1-1* most likely represents a knockout mutant and *osfdml1-2* is more likely to be a knockdown mutant. Both *osfdml1* mutant alleles appeared recessive from the genetic analysis of *osfdml1-1* and *osfdml1-2* backcrossed with the wild-type Hwayoung and Nipponbare cultivars, respectively. In both cases, the F1 heterozygous plants showed normal spikelets but the segregated homozygous plants from F2 progenies displayed floral defects (Supplemental Fig. S2).

Both *osfdml1* mutants displayed no visible differences during vegetative development compared with the wild type. Even though both mutants showed no obvious change in primary branch number, the numbers of secondary branches statistically decreased in the mutants (Supplemental Fig. S4, A–D). The number of secondary branches was ~11.7 in *osfdml1-1* compared with 14.3 in wild-type Hwayoung and 6.0 in *osfdml1-2* compared with 8.3 in wild-type Nipponbare (Supplemental Fig. S4E). These values differ from that of *osmads6*, in which no defects of inflorescence branches were found. We observed that ~33.3% of *osfdml1-1* spikelets displayed defects in palea, lodicule, and pistil development (Supplemental Table S3). Compared with the wild-type plants, ~3.4% of the spikelets of *osfdml1-1* formed wider lemma-like paleae with abnormal marginal region of palea (MRP) tissues in whorl 1 and MRP-like structures and extra lodicules in whorl 2 (Fig. 3, A–C; Supplemental Table S3). Scanning electron microscopy revealed that the cell morphology in the margins of lemma-like palea was converted to that of the body region of the palea (BOP) (Fig. 3B). Normally, the MRP-like structures fused with lodicules (Fig. 3C). Approximately 9.2% of *osfdml1-1* spikelets developed extra lodicules adjacent to the palea in whorl 2 (Fig. 3, D and E; Supplemental Table S3). In contrast to the wild-type pistil normally containing two stigmas, and one locule with one ovule covered by two layers of integuments and one embryo sac (Irish et al., 2003; Tanaka et al., 2014; Fig. 3, F and G), ~20.7% of *osfdml1-1* pistils developed three stigmas, of which ~8.6% showed abnormal exposed ovules (Fig. 3, H–K; Supplemental Table S3). Occasionally, the defective pistils developed two carpels fused together (Fig. 3K). In addition, similar defects were observed in *osfdml1-2* spikelets (Supplemental Fig. S3; Supplemental Table S4). These observations suggest that *OsFDML1* can specify floral organ identity, including palea, lodicule, and pistil, and floral meristem determination in rice (Fig. 3, L and M). Given the similarity between *osfdml1* and *osmads6* in spikelet phenotypes, we proposed that *OsFDML1* and *OsMADS6* genetically function in the same pathway during rice spikelet development.

Ectopic Expression of *OsFDML1* Causes Abnormal Floral Development

To further clarify the function of *OsFDML1*, we constructed *OsFDML1*-overexpressing transgenic (termed as OET6) plants driven by the constitutive CaMV 35S promoter. The expression of *OsFDML1* increased significantly in the spikelets of OET6 lines, which displayed ~25% of floral defects (Fig. 4, G and H). Compared with the wild-type palea, the OET6 developed a slightly wider palea with ectopic MRP tissues (Fig. 4, A–D). Paraffin section observation from OET6 lines showed that the ectopic MRP structures of OET6 developed an additional vascular bundle and additional BOP-like tissues composed of silicified cells, fibrous sclerenchyma, spongy parenchyma, and vacuolated inner surface; the MRP tissues showed a smooth epidermis lacking silicified thickening (Fig. 4, E and F). Moreover, scanning electron microscopy showed chimeric MRP/BOP-like mixed tissues extending into the MRP structures in OET6 palea (Fig. 4D). These findings suggest that *OsFDML1* plays a key role in the establishment of palea identity, similar to that of *OsMADS6*.

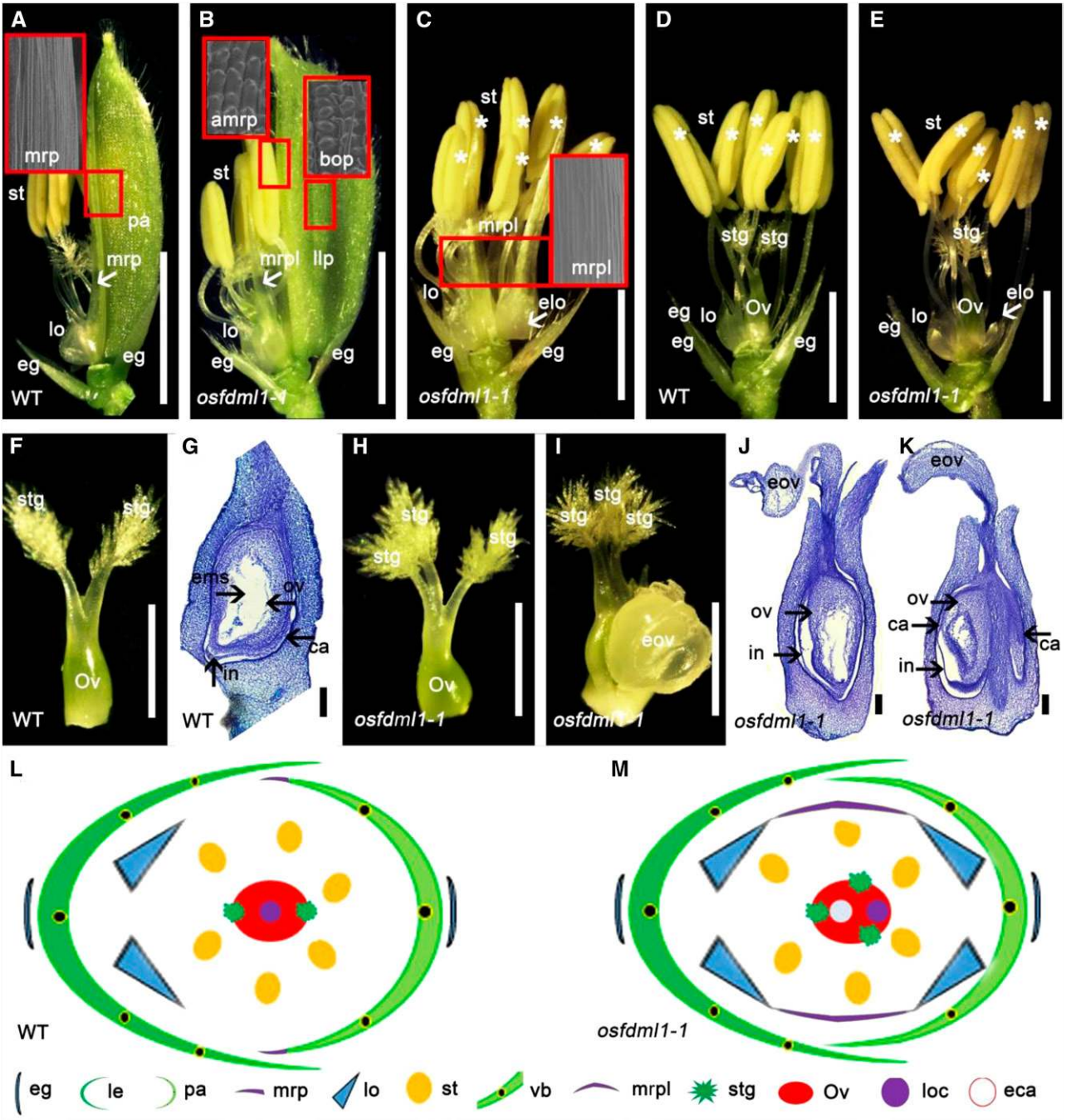

Figure 3. Phenotypes of the wild-type and *osfdml1-1* spikelets. A, Wild-type spikelet (genetic background Hwayoung) with dissected lemma. Arrowhead indicates the MRP structure. The red rectangles indicate the position of scanning electron microscopy and the cell identity of the MRP structure. B, *osfdml1-1* spikelets developing a lemma-like palea in whorl 1 and MRP-like structures in whorl 2. Arrowhead indicates the MRP-like structure. The red rectangles indicate the positions of scanning electron microscopy and the cell identity of the BOP and abnormal MRP structures. C, *osfdml1-1* spikelet with dissected lemma and the lemma-like palea showing extra lodicules and MRP-like structure in whorl 2. Arrowhead indicates the extra lodicules in the palea side. The red rectangles indicate the positions of scanning electron microscopy and the cell identity of the MRP-like structure. D, Wild-type spikelet with lodicules in lemma side, six stamens, and one pistil with two stigmas. Asterisks indicate the stamens. E, *osfdml1-1* spikelets showing extra lodicules in palea side. Arrowhead indicates the extra lodicules in palea side. Asterisks indicate the stamens. F, Wild-type pistil with two stigmas. G, Vertical section of the wild-type ovary. Arrowheads indicate the carpel, integument, ovule, and embryo sac. H, *osfdml1-1* pistil with three stigmas. I, *osfdml1-1* pistil with three stigmas and an exposed ovule. J and K, Vertical section of the *osfdml1-1* ovary. Occasionally two ovaries fused together (K). Arrowheads indicate the carpel, integument, and ovule. L and M, Diagrams of the wild-type and *osfdml1-1* spikelets. eg, Empty glum; pa, palea; llp, lemma-like palea; st, stamen; lo, lodicule; elo, extra lodicules; mrp, marginal region of palea; mrpl,

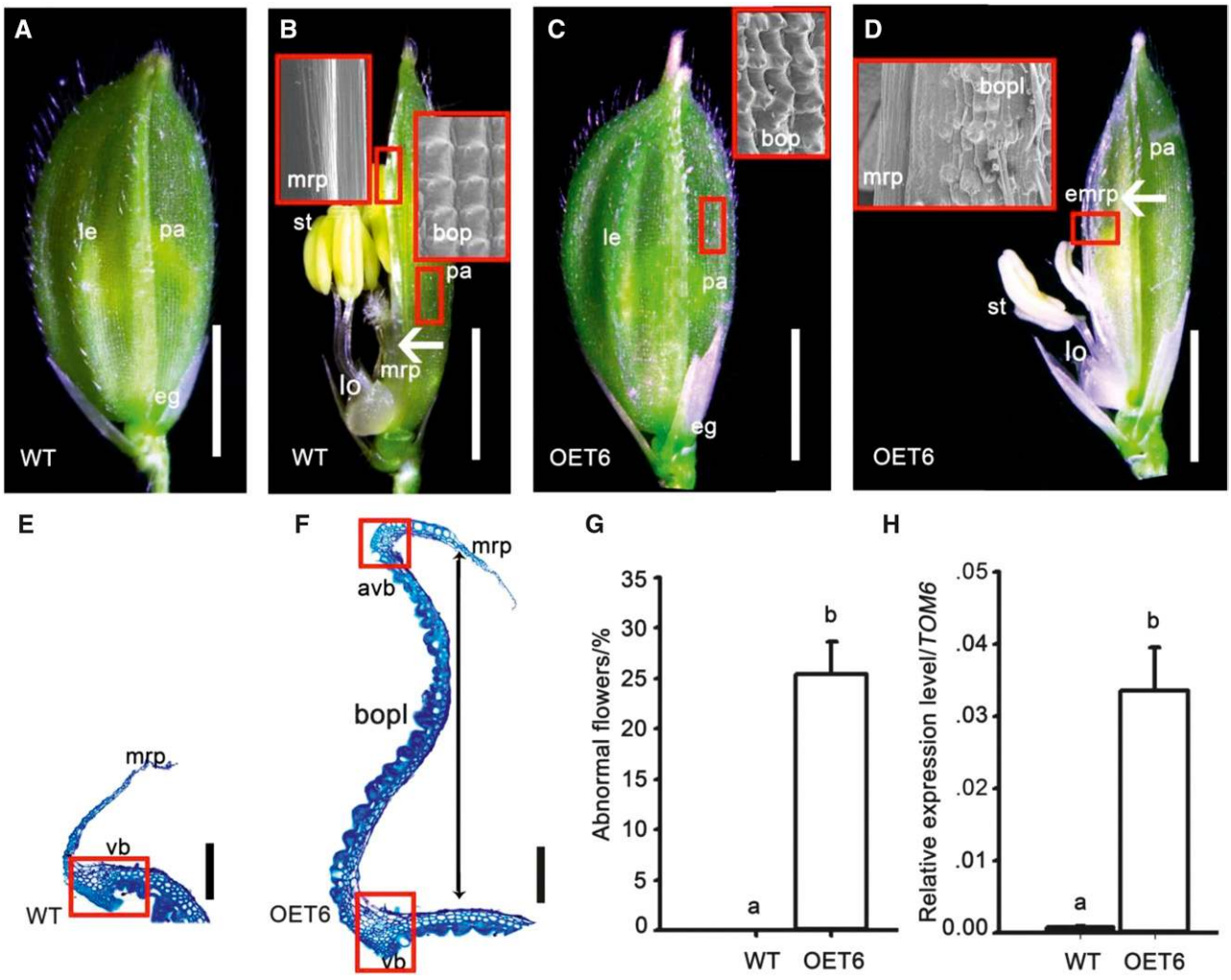

Figure 4. Phenotypes of *OsFDML1* ectopic-expressed spikelets. A and B, Wild-type spikelet (A) with dissected lemma (B). Arrowhead indicates the MRP structure. The red rectangles indicate the positions of scanning electron microscopy and the cell identity of the BOP and MRP structures. C and D, Phenotype of *OsFDML1* overexpressing spikelet (C) with ectopic wider MRP structure (D). Arrowhead indicates the ectopic MRP structure. The red rectangles indicate the position of scanning electron microscopy and the cell identity of the BOP, BOP-like, and MRP structures. E and F, Cross section of the wild-type MRP (E) and the ectopic wider MRP structure of OET6 (F). The vascular bundles are marked by red rectangles. Double-headed arrow indicates the additional BOP-like structure. G, Statistical analysis of abnormal flowers of the wild-type and OET6 inflorescences. All data are means ± SD ($n \geq 5$). H, Relative expression level of *OsFDML1* of the wild-type and OET6 spikelet. All data are means ± SD ($n \geq 3$). Letters a and b represented statistical significance, $P < 0.05$. eg, Empty glume; le, lemma; pa, palea; mrp, marginal region of palea; emrp, ectopic mrp structure; bop, body of palea; bopl, bop-like structure; lo, lodicule; st, stamen; vb, vascular bundle; avb, additional vascular bundle. Bars = 2 mm in A to D and 100 μm in E and F.

OsFDML1 Forms Heterodimers with Its Close Paralog OsFDML2

Sequence analysis showed that 10 members of OsFDML1-like genes were present in rice. Within the subgroup containing OsFDML1, the four paralogs (OsFDML1/2/3/4) exhibited high sequence similarity and contained the conserved domains of XS and XH (Fig. 5A). Given that the homolog in Arabidopsis INVOLVED IN DE NOVO 2/RNA-directed DNA methylation 12 (IDN2/RDM12) functions as homodimers or heterodimers with its paralogs IDN2-like 1 (IDN2L1)/IDN2 PARALOG 1 (IDP1)/FDM1, and IDN2L2/IDP2/

Figure 3. (*Continued.*)
mrp-like structure; bop, body of palea; amrp, abnormal mrp structure; Ov, ovary; stg, stigma; ov, ovule; in, integument; ems, embryo sac; ca, carpel; eov, exposed ovule; vb, vascular bundle; loc, locule; eca, extra carpel. Bars = 2 mm in A and B, 1 mm in C to E, 500 μm in F, H, and I, and 100 μm in G, J, and K.

FDM2 involved in the RdDM pathway in vivo (Ausin et al., 2012; Xie et al., 2012a,b; Zhang et al., 2012), we tested whether OsFDML1 could form protein complexes with its close paralogs in the same subgroup. Yeast two-hybrid analysis showed that only one paralog OsFDML2 could interact with OsFDML1 and that OsFDML1 could not form homodimers (Fig. 5B). To further confirm the interaction between OsFDML1 and OsFDML2, we performed a bimolecular fluorescence complementation (BiFC) assay in rice protoplasts and proved that OsFDML1 indeed interacted with its close paralog OsFDML2 in vivo (Fig. 5C).

In addition, we found that *OsFDML2* is mainly expressed in the spikelet, particularly high in the pistil, which overlaps with *OsFDML1* (Supplemental Fig. S6). Furthermore, both the fused proteins of eGFP-OsFDML1 and eGFP-OsFDML2 were shown to be localized specifically in the nucleus of rice protoplasts (Fig. 5D).

DISCUSSION

Rice *OsMADS6* belongs to the ancient *AGL6* gene family, found in both gymnosperms and angiosperms, which plays roles in flower development in monocots and core eudicots (Ohmori et al., 2009; Reinheimer and Kellogg, 2009; Li et al., 2010; Dreni and Zhang, 2016). The rice genome contains two *AGL6*-like genes, *OsMADS6* and *OsMADS17*, which are involved in flower development (Ohmori et al., 2009; Li et al., 2010; Dreni and Zhang, 2016). *OsMADS6* is expressed in the floral meristem, palea primordia, lodicule, and carpel primordia, and with maturation of the spikelet, *OsMADS6* transcripts are detectable in the ovule and integument (Ohmori et al., 2009; Li et al., 2010; Zhang et al., 2010). Mutation of *OsMADS6* caused severe defects in the spikelet, such as widened palea without MRP tissues, ectopic elongated lodicules and glume-like structures, and multiple pistils with multiple stigmas and independent or fused carpels, representing *SEP*-like function (Ohmori et al., 2009; Li et al., 2010; Zhang et al., 2010; Duan et al., 2012; Dreni and Zhang, 2016). However, given that *OsMADS6* genetically interacts with the floral homeotic genes *SPW1*, *OsMADS3*, *OsMADS1*, *OsMADS7*, and *OsMADS8* and directly regulates *OsMADS58* in specifying floral organ identity and meristem determination (Li et al., 2010, 2011), it remains largely unknown how *AGL6* members regulate flower development.

In this study, we elucidated that *OsFDML1* is a direct downstream target of OsMADS6, as evidenced by the down-regulation of *OsFDML1* in *osmads6* young spikelets and increased expression of *OsFDML1* in transgenic plants when expression of *OsMADS6* is ectopically induced (Fig. 1, A and B). In addition, we proved the direct binding by ChIP-PCR, yeast one-hybrid, and dual-LUC assays (Fig. 1, C–E). *OsFDML1* was mainly expressed in the palea primordia, carpel primordia, and ovule (Fig. 2, C–F), overlapping with the expression of *OsMADS6* (Ohmori et al., 2009; Li et al., 2010; Dreni and Zhang, 2016). The *osfdml1* mutants exhibited lemma-shaped paleae without MRP tissues, increased number of stigmas, occasionally fused carpels, and indeterminate floral meristem, partially phenocopying the role of OsMADS6 in rice floral organ identity specification and meristem determination. The contribution of *OsFDML1* to palea identity specification is demonstrated by the defective palea in *osfdml1* with the lateral outgrowth of BOP in whorl 1 and MRP-like structures in whorl 2 (Fig. 3, B and C; Supplemental Fig. S3, B and C), and transgenic plants overexpressing *OsFDML1* displayed abnormal palea phenotypes with lateral outgrowth of BOP (Fig. 4, D and F). Recent studies indicate that the palea may represent the fusion of three originally distinct organs that evolved into the two lateral MRP and the BOP (Reinheimer and Kellogg, 2009; Lombardo and Yoshida, 2015). Based on the disruption of MRP and BOP formation in *osfdml1* mutants and OET6, we expect that some boundary control factors may determine the fusion of MRP and BOP tissues. For example, the rice mutant *degenerated hull1*, which contains the mutation of a lateral organ boundary domain gene (Li et al., 2008), developed extra MRP-like organs in inner whorls with degenerative lemma and palea (Li et al., 2008). *RETARDED PALEA1* (*REP1*) encodes a *CYCLOIDEA*-like protein, which specifies palea identity and development (Yuan et al., 2009). It is important to determine the relationship of *OsFDML1* with *DH1* and *REP1* in specifying palea identity. Consistent with the regulatory role of *OsMADS6*, *osfdml1* developed abnormal pistils, including those with three stigmas and exposed ovules, which occasionally had two carpels fused together (Fig. 3, H–K). Similarly, *osmads6* mutants produced multiple pistils with multiple stigmas and independent or fused carpels (Ohmori et al., 2009; Li et al., 2010; Zhang et al., 2010). In maize, *bearded-ear* encoding the *AGL6-like* MADS box gene *zea agamous3* exhibited protruding nucellus (Thompson et al., 2009).

The *osfdml1* mutants have weaker floral defects than the *osmads6* mutants because OsMADS6 may have multiple regulatory targets, which remain to be discovered. Alternatively, there is functional redundancy of *OsFDML1* because rice has nine other homologs of *OsFDML1* that contain the featured XS and/or XH domains (Chen and Bennetzen, 1996; Bateman, 2002). However, few of them have been functionally characterized due to lack of knockout or knockdown mutants. In contrast to rice *osfdml1* mutants, the single mutation *idn2/rdm12* and the sextuple mutations *idn2-3 fdm1-1 idp2-1 fdm3-2 fdm4-2 fdm5-2* cause no obvious developmental defects, and they only result in minor changes in DNA methylation (Ausin et al., 2009; Zheng et al., 2010; Butt et al., 2014), suggesting strong redundancy of closely related proteins in Arabidopsis. These results indicate that members of this family may undergo a certain degree of functional diversification between monocots and eudicots during evolution. In Arabidopsis, the *SGS3*-like *IDN2/RDM12*, functioning

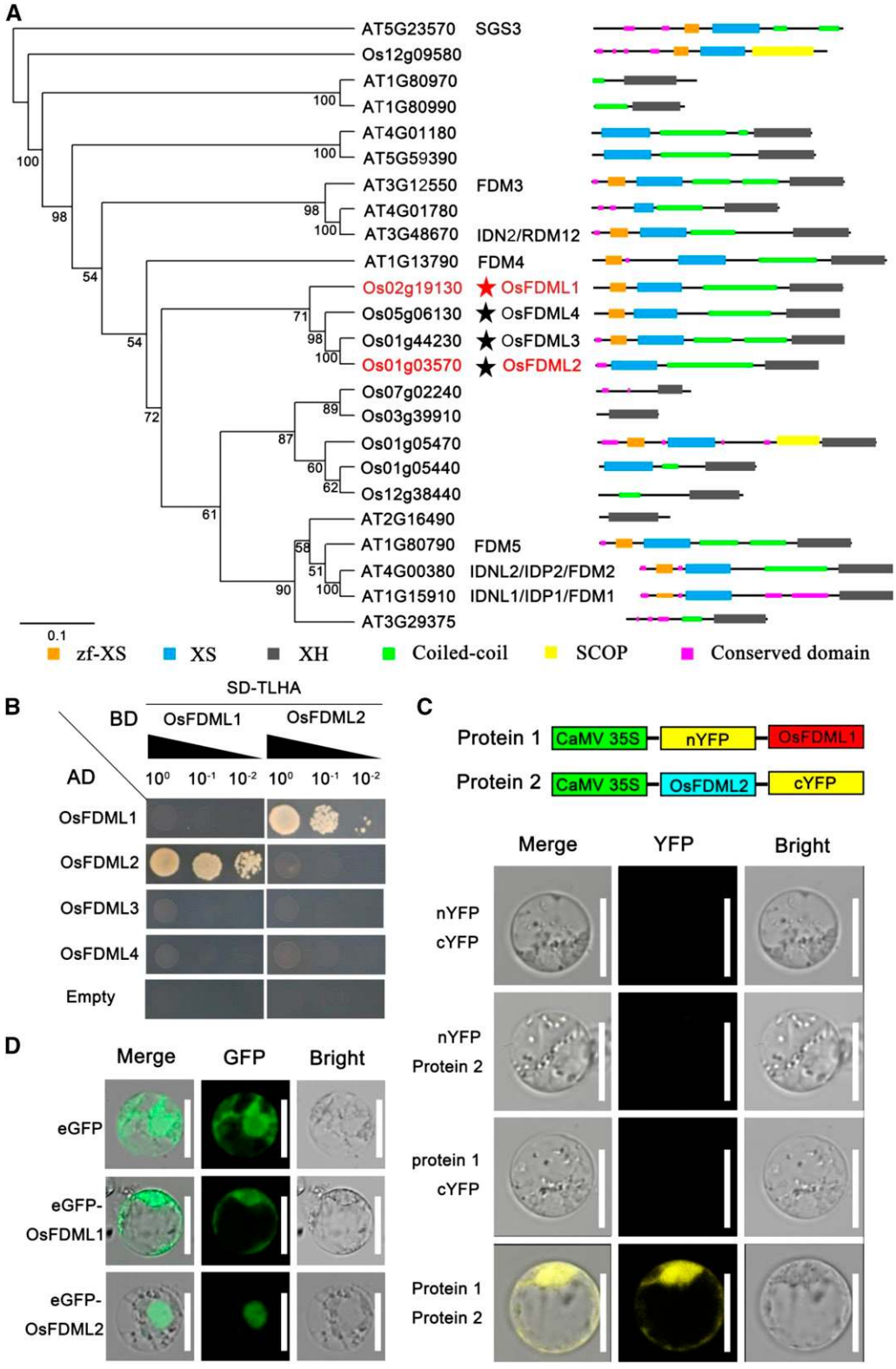

Figure 5. OsFDML1 functions as heterodimers with its close paralog OsFDML2. A, The neighbor-joining phylogenetic tree of *OsFDML1* with homologs in rice and Arabidopsis. The bootstrap values (%) based on 100 replicates are marked at the branching points. The scale bar indicates the number of nucleotide substitutions per site. OsFDML1 and the interacting protein OsFDML2 are marked in red. The red star indicates *OsFDML1*. The black stars indicate the other three paralogs OsFDML2, OsFDML3, and OsFDML4 in rice belonging to the same subgroup. B, OsFDML1 interacts with its close paralog OsFDML2 by

as a homodimer and heterodimer in vivo with its two paralogs IDNL1/IDP1/FDM1 and IDNL2/IDP2/FDM2, potentially stabilizes the AGO4-delivered small interfering RNA to the correct chromatin sites, and is an important component in the RdDM pathway (Mourrain et al., 2000; Bateman, 2002; Ausin et al., 2012; Finke et al., 2012; Xie et al., 2012b; Zhang et al., 2012). This study revealed that rice OsFDML1 functions as a heterodimer by interacting with its close paralog OsFDML2 in both yeast two-hybrid and BiFC assays (Fig. 5, B and C), mimicking the homologs in Arabidopsis, which suggests that the genes responsible for the functions of this family might have been conserved in the evolution of flowering plants. Given that *IDN2/RDM12* in Arabidopsis contributes to DNA methylation in the RdDM pathway, it would be interesting to test whether *OsFDML1* regulates flower development via epigenetic modifications.

Moreover, in Arabidopsis, floral MADS box genes were suggested to regulate the expression of genes associated with chromatin structure remodeling (Yan et al., 2016). For example, Arabidopsis E-class protein SEP3 was identified to recruit SWITCH 2/SUC NONFERMENTING2 (SWI2/SNF2) chromatin-remodeling ATPases BRAHMA and SPLAYED to the regulatory loci of *AP3* and *AG*, resulting in the induction of their expression by overcoming Polycomb repression (Smaczniak et al., 2012; Wu et al., 2012). In Arabidopsis, IDN2 dimers were shown to physically interact with SWI3B, a core subunit of SWI/SNF ATP-dependent chromatin-remodeling complex, which positioned nucleosomes and affected transcription (Zhu et al., 2013). Thus, our findings provide key insights into the regulatory network of *AGL6*-like genes and may illustrate a new link between genetics (*AGL6*) and epigenetics, adding to the current understanding of epigenetic mechanisms and chromatin structure in rice flower development.

In summary, based on the observation of the spikelet phenotype of plants with altered expression of *OsFDML1* and its expression pattern, as well as the heterodimers formed by OsFDML1 and its close paralog OsFDML2, we have presented a model in which the transcription factor OsMADS6 directly activates the expression of *OsFDML1*, and the protein OsFDML1 forms heterodimers with OsFDML2 to regulate rice flower development, probably via DNA methylation modification (Fig. 6).

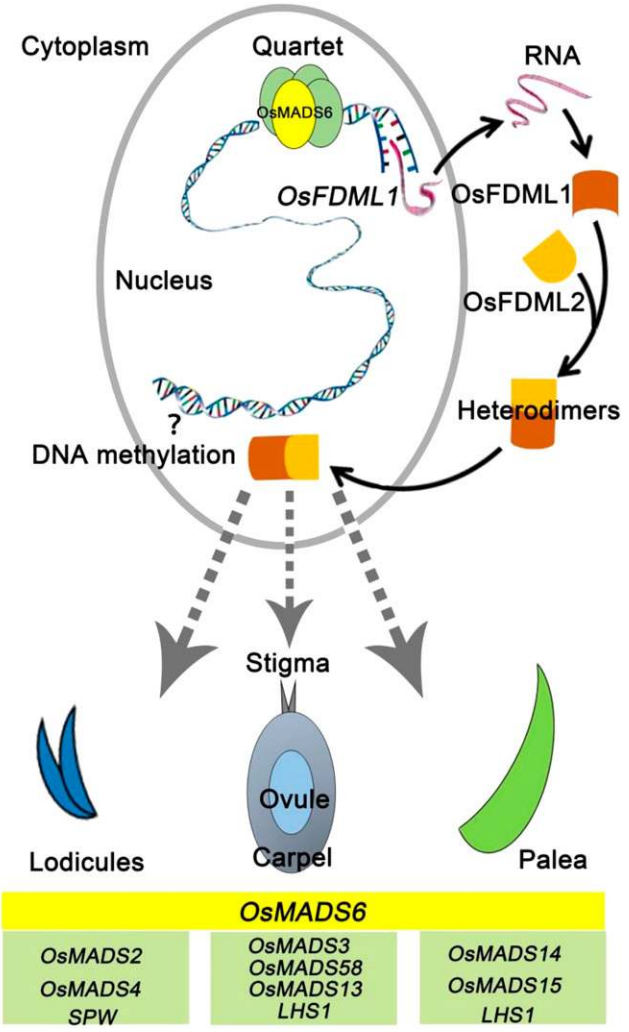

Figure 6. An updated model for the regulation of palea, lodicule, and pistil development by OsMADS6 via direct activation of *OsFDML1*. OsFDML1 functions as heterodimers with its close paralog OsFDML2.

MATERIALS AND METHODS

Plant Materials

The recessive mutants *osfdml1-1* (PFG_1C-03064, 'Hwayoung') and *osfdml1-2* (NE4801, 'Nipponbare') were obtained from the Rice Genome Resource Center, National Institute of Agrobiology Sciences (Japan) (Miyao et al., 2003) and Rice T-DNA Insertion Sequence Database (Korea), respectively. The mutant *osmads6-1* (Li et al., 2010) with genetic background 9522 (*Oryza sativa* ssp. *japonica*) was a wild-type plant. The transgenic plants InDE6 were continuously grown and harvested for three planting seasons, and the T3 transgenic seeds were used for the OsMADS6-induced expression experiment. The OET6 transgenic plants were continuously grown and harvested for T2 transgenic plants and phenotype observation and floral tissue collection were performed. All rice plants were grown in the paddy field. The *Nicotiana benthamiana* plants were grown at 23°C under 16-h daylight conditions in a greenhouse. The phenotypes of *osfdml1* and transgenic plants OET6 were sensitive to the environment, and all of the phenotypes reported in this study were observed twice successively in the paddy field under climatic conditions reported at www.tianqi.com and www.richurimo.51240.com (Supplemental Fig. S5).

ChIP-qPCR and Enrichment Analysis

Approximately 1 g of wild-type rice inflorescence 2 to 8 mm in length was cross-linked by 1% formaldehyde and sonicated four times for 10 s each,

Figure 5. (*Continued*.)
yeast two-hybrid assay. C, OsFDML1 interacts with OsFDML2 in vivo by BiFC assay in rice protoplast. D, OsFDML1 localizes in nucleus and cytoplasm, and OsFDML2 localizes in nucleus in rice protoplast. Bars = 10 μm in C and D.

with a 30-s break after each round of sonication, using an Ultrasonic Crasher Noise Isolating Chamber (Scientz) at 100 W; this yielded chromatin DNA with a size of <500 bp. ChIP of the OsMADS6-DNA complexes followed the protocol of Li et al. (2011). The precipitated and recovered DNA was diluted with 100 µL of double-distilled water, and each reaction was performed in three biological replicates. Primer pairs FDML1LP1 + FDML1RP1 and FDML1LP2 + FDML1RP2 were used for qPCR (Supplemental Table S5). The reactions were performed using SYBR Green Master mix (Bio-Rad) on a real-time PCR instrument (Bio-Rad). The calculation of relative enrichment of the fragments with the putative CArG motifs followed the method suggested by Li et al. (2011).

RT-qPCR

We extracted total RNA from roots, stems, leaves, young inflorescences, and dissected lemmas, paleae, stamens, and pistils using Trizol reagent (Invitrogen) according to the manufacturer's instructions. About 1 µg total RNA was reverse transcribed with PrimeScript RT reagent Kit with gDNA Eraser (Takara). RT-qPCR was performed using SYBR Green Master Mix (Bio-Rad) on a real-time PCR instrument (Bio-Rad). Specific primers were designed and validated by melt curve and standard curve (R^2 = 0.9996, E = 0.957 for FDML1F and FDML1R; R^2 = 0.9998, E = 0.991 for FDML2F and FDML2R primer pairs) first before being applied to detect gene expression. We collected ~30 1- to 2-cm-long roots from 15 seedlings, two 1-cm-long stems from two plants, one 2-cm-long leaves from one plant, 10 2-mm-long inflorescences, six 2- to 3-mm-long inflorescences, four 4- to 7-mm-long inflorescences, 15 dissected lemmas, 15n dissected paleae, 60 stamens, and 60 pistils for one biological replicate of different tissues. Data shown in this research were summarized from three biological replicates and three PCR replicates normalized to *ACTIN* expression.

OsMADS6-Induced Expression Experiment

We germinated ~200 seeds of the wild-type and InDE6 T3 transgenic plants in water for ~1 week. The young seedlings were divided into two equally sized groups and treated with 5 µM β-estradiol and the solvent DMSO, respectively. Thereafter, we collected 0.5- to 1-cm root tips from 10 young seedlings for each biological repeat at 0, 12, and 24 h. Each sample consisted of three biological replicates for total RNA extraction. The primers were FDML1F and FDML1R for *OsFDML1* (Supplemental Table S5). RT-qPCR was performed using a real-time RCR instrument (Bio-Rad) with SYBR green Master mix (Bio-Rad). The relative expression levels of *OsFDML1* and *OsMADS6* were normalized relative to *ACTIN* expression.

Yeast One-Hybrid Assay

We cloned the full-length *OsMADS6* cDNA to vector pGADT7 and the 102-bp DNA fragment containing the putative CArG motif to vector pHIS2, respectively, using the primer pair pHIS2F1F and pHIS2F1R (Supplemental Table S5). The yeast strain Y187 was then cotransformed and cultured at 30°C for 2 to 3 d on solid dropout media, SD-TL, with the empty vectors as negative controls. We chose three independent positive strains, incubated in liquid SD-TL media overnight and diluted to 1/10 in a gradient. Finally, we drew 5 µL of cotransformed host strains on the solid SD-TLH media with 20 nM 3-AT (Zhang et al., 2012).

Dual-Luciferase Assay

The LUC transactivation (dual-LUC) method was modified from the protocol described by Bennett et al. (1996). The effector OsMADS6-Flag was prepared by cloning the full length of OsMADS6 cDNA containing the primer pair pGM6F and pGM6R into the modified vector pGreenII-0000 with Flag driven by the CaMV 35S promoter (Supplemental Table S5). Both the empty vector and the modified vector with Flag were used as negative controls. The reporter *OsFDML1pro:LUC* was constructed by cloning the 3795-bp *OsFDML1* genome sequence upstream of the ATG with primers pG0800F1F and pG0800F1R into the vector *pGreenII-0800-LUC* (Supplemental Table S5). The empty vector was used as a control.

The transformation of all the effectors and reporters followed the protocol of Li et al. (2014). *Agrobacterium tumefaciens* cultured overnight was collected and resuspended in Murashige and Skoog liquid medium to OD_{600} values of 0.6 to 0.8. The mixture with the effector and reporter strain at a ratio 4:1 was incubated for 3 h at room temperature with 10 mM MES and 200 µM acetosyringone and infiltrated into young *N. benthamiana* leaves, and the plants were kept for 48 h under weak light conditions. Four biological replicates were performed for each sample. The LUC/REN signals were calculated using dual-LUC assay solutions (Promega) on a luminometer (Promega).

Genotyping of *osfdml1* Mutants and *OsFDML1* Expression Level Test

Primer combinations for *osfdml1-1* were LD82 + LD83 and LD82 + Tos7, and those for *osfdml1-2* were LD55 + LD56 and LD56 + Osp79 (Supplemental Table S5). The precise positions of *Tos17* and T-DNA were determined by PCR sequencing. To test the expression change of *OsFDML1* in two *osfdml1* mutants, we designed primers (i.e. F1, R1, F2, R2, and F3) for different sites according to the position of *Tos17* and T-DNA (Supplemental Table S5).

Rice Transformation

For *OsFDML1* overexpression, the full-length cDNA of *OsFDML1* generated with primers pCAMF1F and pCAMF1R was cloned into vector pCAMBIA1301 driven by the CaMV 35S (Supplemental Table S5). We cultured the sheared young spikelets at 28°C under dark conditions for 12 to 15 d until the callus grew. The transformation of *35Spro:OsFDML1* was introduced to the wild-type callus by the *A. tumefaciens*-mediated method using hygromycin for selection.

Histochemical and Scanning Electron Microscopy Observation

All of the materials were fixed in formalin-acetic acid-alcohol solution with 3.7% formaldehyde at 4°C overnight, dehydrated in graded ethanol, infiltrated with Histo-Clear II (National Diagnostics), and embedded in paraffin (Sigma-Aldrich; the same products and procedure for in situ hybridization experiment). Sections of the tissues (8-µm thick) were prepared using a microtome (Leica), stained with 0.1% toluidine blue, and photographed under a bright-field microscope (Nikon). Scanning electron microscopy images were acquired using a scanning electron microscope (JEOL).

In Situ Hybridization

Tissues were fixed in formalin-acetic acid-alcohol solution with 3.7% formaldehyde at 4°C for 2 h and dehydrated in a series of different ethanol concentrations. Tissue sections (6- to 8-µm thick) were prepared following the same procedure used for histochemical observations.

The probes were amplified with primers F1F + F1T7R (henceforth referred to as "antisense probe") and F1T7F + F1R (henceforth referred to as "sense probe"), respectively. F1T7F and F1T7R were designed by adding 20-bp T7 promoter sequences TAATACGACTCACTATAGGG to the 5′ end of the primers (Supplemental Table S5). The antisense and sense probes were labeled with digoxigenin using an in vitro transcription kit (Roche) with T7 polymerase. The procedures for in situ hybridization and digoxigenin signal detection followed the protocol described by Dreni et al. (2007).

Yeast Two-Hybrid Assay

To perform the yeast two-hybrid analysis, we first cloned the full-length cDNAs of *OsFDML1*, *OsFDML2*, *OsFDML3*, and *OsFDML4* into vectors pGADT7 and pGBKT7, respectively. Subsequently, we cotransformed the corresponding pGADT7 and pGBKT7 constructs into the yeast strain AH109 and cultured the yeast on solid dropout media SD-TL at 30°C for 2 to 3 d. The positive strains were incubated in liquid SD-TL media overnight and collected by centrifugation, and the serial decimal dilution was used for spot assay on dropout media SD-TLHA (the main procedures followed the yeast protocol handbook from Clontech). The GAL4-AD-OsFDML1-fused protein and GAL4-BD-OsFDML2-fused protein activated the expression of the reporter gene *HIS3*, which was confirmed by the results from GAL4-AD-OsFDML2-fused protein and GAL4-BD-OsFDML1 expression. Primers for these constructs are listed in Supplemental Table S5.

Subcellular Localization of OsFDML1 in Protoplast

The full-length cDNAs of *OsFDML1* and *OsFDML2*, amplified with the primer combinations pA7F1F + pA7F1R and pA7F2F + pA7F2R, respectively, were cloned into vector pA7 encoding GFP driven by CaMV 35S (Supplemental Table S5). The recombinant plasmid expressing eGFP-OsFDML1 and eGFP-OsFDML2 fused proteins was introduced into rice protoplasts following the protocol described by Bart et al. (2006). The images were visualized using a confocal microscope (Leica).

BiFC Assay in Protoplast

The full-length cDNAs of *OsFDML1* and *OsFDML2* were cloned into vectors pSAT-cEYFP-c1 and pSAT-nEYFP-c1, respectively. All the steps for the BiFC assay followed the protocol of Zhang et al. (2011).

Phylogenetic Analysis

The 119 homologs were obtained using the full-length protein sequence of OsFDML1 as the query to search in the Phytozome database (http://phytozome.jgi.doe.gov) and Congenie database (http://congenie.org). The 24 protein sequences from Arabidopsis and rice were multiple-aligned by MAFFT (http://mafft.cbrc.jp/alignment/server) and kept the conserved XS-XH domain as determined by Genedoc (Nicholas et al., 1997). The neighbor-joining phylogenetic tree was constructed following a method described previously (Pelucchi et al., 2002). The bootstrap values (%) based on 100 replicates are marked at the branching points.

Statistical Analysis

Statistical works were run with SigmaPlot 12.0. All data were expressed as means ± SD ($n \geq 3$). Statistical significance level of $P < 0.05$ between different sample groups was tested using ANOVA.

Accession Numbers

Sequence data from this article can be found in the Rice Genome Annotation Project and the Arabidopsis Information Resource data libraries under the following accession numbers: *OsFDML1* (Os02g0293300), *OsFDML2* (Os01g0126600), *OsFDML3* (Os01g0633200), *OsFDML4* (Os05g0153200), *SGS3* (AT5G23570), *IDN2/RDM12* (AT3G48670), *FDM1* (AT1G15910), *FDM2* (AT4G00380), *FDM3* (AT3G12550), *FDM4* (AT1G13790), and *FDM5* (AT1G80790). Accession numbers for the sequences used in the phylogenetic analysis are listed on the tree.

Supplemental Data

The following supplemental materials are available.

Supplemental Figure S1. Identification of two allelic *osfdml1* mutants.

Supplemental Figure S2. Spikelet phenotypes of heterozygous and homozygous *osfdml1-1* and *osfdml1-2* mutants.

Supplemental Figure S3. Phenotypes of wild-type and *osfdml1-2* spikelets.

Supplemental Figure S4. The phenotype and statistical analysis of the primary branch and secondary branch of the mutant inflorescences.

Supplemental Figure S5. The climatic conditions of mutant growth in the field in 2017.

Supplemental Figure S6. The expression pattern of *OsFDML2* in the wild type.

Supplemental Table S1. List of genes putatively encoding transcription factors and kinases with the changed expression in *osmads6-1* from microarray analysis by Li et al. (2011).

Supplemental Table S2. Homologs of *OsFDML1* in 14 species of terrestrial plants.

Supplemental Table S3. Number of floral organs in whorls 1, 2, 3, and 4 of *osfdml1-1*.

Supplemental Table S4. Number of floral organs in whorls 1, 2, 3, and 4 of *osfdml1-2*.

Supplemental Table S5. Sequence information of primers.

ACKNOWLEDGMENTS

We thank Dr. Ludovico Dreni for assisting in data analysis; Zhijing Luo, Mingjiao Chen, and Zibo Chen for rice materials planting; Yun Hu for providing OsMADS6 rabbit polyclonal antibody and for InDE6 transgenic plant construction; and Changsong Yin and Jie Wang for their excellent assistance on in situ hybridization.

Received January 9, 2018; accepted April 18, 2018; published May 1, 2018.

LITERATURE CITED

Agrawal GK, Abe K, Yamazaki M, Miyao A, Hirochika H (2005) Conservation of the E-function for floral organ identity in rice revealed by the analysis of tissue culture-induced loss-of-function mutants of the OsMADS1 gene. Plant Mol Biol **59**: 125–135

Ambrose BA, Lerner DR, Ciceri P, Padilla CM, Yanofsky MF, Schmidt RJ (2000) Molecular and genetic analyses of the silky1 gene reveal conservation in floral organ specification between eudicots and monocots. Mol Cell **5**: 569–579

Arora R, Agarwal P, Ray S, Singh AK, Singh VP, Tyagi AK, Kapoor S (2007) MADS-box gene family in rice: genome-wide identification, organization and expression profiling during reproductive development and stress. BMC Genomics **8**: 242

Ausin I, Mockler TC, Chory J, Jacobsen SE (2009) IDN1 and IDN2 are required for de novo DNA methylation in *Arabidopsis thaliana*. Nat Struct Mol Biol **16**: 1325–1327

Ausin I, Greenberg MV, Simanshu DK, Hale CJ, Vashisht AA, Simon SA, Lee TF, Feng S, Española SD, Meyers BC, (2012) INVOLVED IN DE NOVO 2-containing complex involved in RNA-directed DNA methylation in *Arabidopsis*. Proc Natl Acad Sci USA **109**: 8374–8381

Barker NP, Clark LG, Davis JI, Duvall MR, Guala GF, Hsiao C, Kellogg EA, Linder HP, (2001) Phylogeny and subfamilial classification of the grasses (Poaceae). Ann Mo Bot Gard **88**: 373–457

Bart R, Chern M, Park CJ, Bartley L, Ronald PC (2006) A novel system for gene silencing using siRNAs in rice leaf and stem-derived protoplasts. Plant Methods **2**: 13

Bateman A (2002) The SGS3 protein involved in PTGS finds a family. BMC Bioinformatics **3**: 21

Bennett MJ, Marchant A, Green HG, May ST, Ward SP, Millner PA, Walker AR, Schulz B, Feldmann KA (1996) Arabidopsis AUX1 gene: a permease-like regulator of root gravitropism. Science **273**: 948–950

Bommert P, Satoh-Nagasawa N, Jackson D, Hirano HY (2005) Genetics and evolution of inflorescence and flower development in grasses. Plant Cell Physiol **46**: 69–78

Brambilla V, Battaglia R, Colombo M, Masiero S, Bencivenga S, Kater MM, Colombo L (2007) Genetic and molecular interactions between BELL1 and MADS box factors support ovule development in *Arabidopsis*. Plant Cell **19**: 2544–2556

Butt H, Graner S, Luschnig C (2014) Expression analysis of *Arabidopsis* XH/XS-domain proteins indicates overlapping and distinct functions for members of this gene family. J Exp Bot **65**: 1217–1227

Callens C, Tucker MR, Zhang D, Wilson ZA (2018) Dissecting the role of MADS-box genes in monocot floral development and diversity. J Exp Bot

Chen M, Bennetzen JL (1996) Sequence composition and organization in the Sh2/A1-homologous region of rice. Plant Mol Biol **32**: 999–1001

Chen ZX, Wu JG, Ding WN, Chen HM, Wu P, Shi CH (2006) Morphogenesis and molecular basis on naked seed rice, a novel homeotic mutation of OsMADS1 regulating transcript level of AP3 homologue in rice. Planta **223**: 882–890

Coen ES, Meyerowitz EM (1991) The war of the whorls: genetic interactions controlling flower development. Nature **353**: 31–37

Cui R, Han J, Zhao S, Su K, Wu F, Du X, Xu Q, Chong K, Theissen G, Meng Z (2010) Functional conservation and diversification of class E floral homeotic genes in rice (*Oryza sativa*). Plant J **61**: 767–781

Ditta G, Pinyopich A, Robles P, Pelaz S, Yanofsky MF (2004) The SEP4 gene of *Arabidopsis thaliana* functions in floral organ and meristem identity. Curr Biol **14**: 1935–1940

Dreni L, Kater MM (2014) MADS reloaded: evolution of the AGAMOUS subfamily genes. New Phytol **201**: 717–732

Dreni L, Zhang D (2016) Flower development: the evolutionary history and functions of the AGL6 subfamily MADS-box genes. J Exp Bot **67**: 1625–1638

Dreni L, Jacchia S, Fornara F, Fornari M, Ouwerkerk PB, An G, Colombo L, Kater MM (2007) The D-lineage MADS-box gene OsMADS13 controls ovule identity in rice. Plant J **52**: 690–699

Dreni L, Pilatone A, Yun D, Erreni S, Pajoro A, Caporali E, Zhang D, Kater MM (2011) Functional analysis of all AGAMOUS subfamily members in rice reveals their roles in reproductive organ identity determination and meristem determinacy. Plant Cell **23**: 2850–2863

Duan Y, Xing Z, Diao Z, Xu W, Li S, Du X, Wu G, Wang C, Lan T, Meng Z, (2012) Characterization of Osmads6-5, a null allele, reveals that OsMADS6 is a critical regulator for early flower development in rice (*Oryza sativa* L.). Plant Mol Biol **80**: 429–442

Finke A, Kuhlmann M, Mette MF (2012) IDN2 has a role downstream of siRNA formation in RNA-directed DNA methylation. Epigenetics **7**: 950–960

Gao X, Liang W, Yin C, Ji S, Wang H, Su X, Guo C, Kong H, Xue H, Zhang D (2010) The SEPALLATA-like gene OsMADS34 is required for rice inflorescence and spikelet development. Plant Physiol **153**: 728–740

Hu Y, Liang W, Yin C, Yang X, Ping B, Li A, Jia R, Chen M, Luo Z, Cai Q, (2015) Interactions of OsMADS1 with floral homeotic genes in rice flower development. Mol Plant **8**: 1366–1384

Irish EE, Szymkowiak EJ, Garrels K (2003) The wandering carpel mutation of *Zea mays* (Gramineae) causes misorientation and loss of zygomorphy in flowers and two-seeded kernels. Am J Bot **90**: 551–560

Itoh J, Nonomura K, Ikeda K, Yamaki S, Inukai Y, Yamagishi H, Kitano H, Nagato Y (2005) Rice plant development: from zygote to spikelet. Plant Cell Physiol **46**: 23–47

Jeon JS, Jang S, Lee S, Nam J, Kim C, Lee SH, Chung YY, Kim SR, Lee YH, Cho YG, An G (2000) *leafy hull sterile1* is a homeotic mutation in a rice MADS box gene affecting rice flower development. Plant Cell **12**: 871–884

Kellogg EA (2001) Evolutionary history of the grasses. Plant Physiol **125**: 1198–1205

Kellogg EA (2015) Inflorescence Structure. In: Flowering Plants, Monocots: Poaceae. The Families and Genera of Vascular Plants **13**: 25–38

Kobayashi K, Maekawa M, Miyao A, Hirochika H, Kyozuka J (2010) PANICLE PHYTOMER2 (PAP2), encoding a SEPALLATA subfamily MADS-box protein, positively controls spikelet meristem identity in rice. Plant Cell Physiol **51**: 47–57

Kyozuka J, Kobayashi T, Morita M, Shimamoto K (2000) Spatially and temporally regulated expression of rice MADS box genes with similarity to *Arabidopsis* class A, B and C genes. Plant Cell Physiol **41**: 710–718

Li A, Zhang Y, Wu X, Tang W, Wu R, Dai Z, Liu G, Zhang H, Wu C, Chen G, Pan X (2008) DH1, a LOB domain-like protein required for glume formation in rice. Plant Mol Biol **66**: 491–502

Li G, Liang W, Zhang X, Ren H, Hu J, Bennett MJ, Zhang D (2014) Rice actin-binding protein RMD is a key link in the auxin-actin regulatory loop that controls cell growth. Proc Natl Acad Sci USA **111**: 10377–10382

Li H, Liang W, Jia R, Yin C, Zong J, Kong H, Zhang D (2010) The AGL6-like gene OsMADS6 regulates floral organ and meristem identities in rice. Cell Res **20**: 299–313

Li H, Liang W, Hu Y, Zhu L, Yin C, Xu J, Dreni L, Kater MM, Zhang D (2011) Rice MADS6 interacts with the floral homeotic genes SUPERWOMAN1, MADS3, MADS58, MADS13, and DROOPING LEAF in specifying floral organ identities and meristem fate. Plant Cell **23**: 2536–2552

Lombardo F, Yoshida H (2015) Interpreting lemma and palea homologies: a point of view from rice floral mutants. Front Plant Sci **6**: 61

Malcomber ST, Kellogg EA (2004) Heterogeneous expression patterns and separate roles of the *SEPALLATA* gene *LEAFY HULL STERILE1* in grasses. Plant Cell **16**: 1692–1706

Malcomber ST, Kellogg EA (2005) SEPALLATA gene diversification: brave new whorls. Trends Plant Sci **10**: 427–435

Miyao A, Tanaka K, Murata K, Sawaki H, Takeda S, Abe K, Shinozuka Y, Onosato K, Hirochika H (2003) Target site specificity of the Tos17 retrotransposon shows a preference for insertion within genes and against insertion in retrotransposon-rich regions of the genome. Plant Cell **15**: 1771–1780

Moon YH, Kang HG, Jung JY, Jeon JS, Sung SK, An G (1999) Determination of the motif responsible for interaction between the rice APETALA1/AGAMOUS-LIKE9 family proteins using a yeast two-hybrid system. Plant Physiol **120**: 1193–1204

Mourrain P, Béclin C, Elmayan T, Feuerbach F, Godon C, Morel JB, Jouette D, Lacombe AM, Nikic S, Picault N, (2000) *Arabidopsis* SGS2 and SGS3 genes are required for posttranscriptional gene silencing and natural virus resistance. Cell **101**: 533–542

Nagasawa N, Miyoshi M, Sano Y, Satoh H, Hirano H, Sakai H, Nagato Y (2003) SUPERWOMAN1 and DROOPING LEAF genes control floral organ identity in rice. Development **130**: 705–718

Nicholas KB, Nicholas HB, Deerfield DWI (1997) Gene-Doc: analysis and visualization of genetic variation. Embnew News **4**: 14

Ohmori S, Kimizu M, Sugita M, Miyao A, Hirochika H, Uchida E, Nagato Y, Yoshida H (2009) MOSAIC FLORAL ORGANS1, an AGL6-like MADS box gene, regulates floral organ identity and meristem fate in rice. Plant Cell **21**: 3008–3025

Pelaz S, Ditta GS, Baumann E, Wisman E, Yanofsky MF (2000) B and C floral organ identity functions require SEPALLATA MADS-box genes. Nature **405**: 200–203

Pelaz S, Gustafson-Brown C, Kohalmi SE, Crosby WL, Yanofsky MF (2001b) APETALA1 and SEPALLATA3 interact to promote flower development. Plant J **26**: 385–394

Pelaz S, Tapia-López R, Alvarez-Buylla ER, Yanofsky MF (2001a) Conversion of leaves into petals in *Arabidopsis*. Curr Biol **11**: 182–184

Pelucchi N, Fornara F, Favalli C, Masiero S, Lago C, Pè ME, Colombo L, Kater MM (2002) Comparative analysis of rice MADS-box genes expressed during flower development. Sex Plant Reprod **15**: 113–122

Pinyopich A, Ditta GS, Savidge B, Liljegren SJ, Baumann E, Wisman E, Yanofsky MF (2003) Assessing the redundancy of MADS-box genes during carpel and ovule development. Nature **424**: 85–88

Prasad K, Parameswaran S, Vijayraghavan U (2005) OsMADS1, a rice MADS-box factor, controls differentiation of specific cell types in the lemma and palea and is an early-acting regulator of inner floral organs. Plant J **43**: 915–928

Preston JC, Kellogg EA (2006) Reconstructing the evolutionary history of paralogous APETALA1/FRUITFULL-like genes in grasses (Poaceae). Genetics **174**: 421–437

Prusinkiewicz P, Erasmus Y, Lane B, Harder LD, Coen E (2007) Evolution and development of inflorescence architectures. Science **316**: 1452–1456

Reinheimer R, Kellogg EA (2009) Evolution of AGL6-like MADS box genes in grasses (Poaceae): ovule expression is ancient and palea expression is new. Plant Cell **21**: 2591–2605

Rudall PJ, Stuppy W, Cunniff J, Kellogg EA, Briggs BG (2005) Evolution of reproductive structures in grasses (Poaceae) inferred by sister-group comparison with their putative closest living relatives, Ecdeiocoleaceae. Am J Bot **92**: 1432–1443

Sang X, Li Y, Luo Z, Ren D, Fang L, Wang N, Zhao F, Ling Y, Yang Z, Liu Y, He G (2012) CHIMERIC FLORAL ORGANS1, encoding a monocot-specific MADS box protein, regulates floral organ identity in rice. Plant Physiol **160**: 788–807

Smaczniak C, Immink RG, Muiño JM, Blanvillain R, Busscher M, Busscher-Lange J, Dinh QD, Liu S, Westphal AH, Boeren S, (2012) Characterization of MADS-domain transcription factor complexes in Arabidopsis flower development. Proc Natl Acad Sci USA **109**: 1560–1565

Tanaka W, Toriba T, Hirano HY (2014) Flower development in rice. Adv Bot Res **72**: 221–262

Theissen G, Saedler H (2001) Plant biology. Floral quartets. Nature **409**: 469–471

Thompson BE, Hake S (2009) Translational biology: from Arabidopsis flowers to grass inflorescence architecture. Plant Physiol **149**: 38–45

Thompson BE, Bartling L, Whipple C, Hall DH, Sakai H, Schmidt R, Hake S (2009) *bearded-ear* encodes a MADS box transcription factor critical for maize floral development. Plant Cell **21**: 2578–2590

Wang H, Zhang L, Cai Q, Hu Y, Jin Z, Zhao X, Fan W, Huang Q, Luo Z, Chen M, Zhang D, Yuan Z (2015) OsMADS32 interacts with PI-like proteins and regulates rice flower development. J Integr Plant Biol **57**: 504–513

Wang K, Tang D, Hong L, Xu W, Huang J, Li M, Gu M, Xue Y, Cheng Z (2010) DEP and AFO regulate reproductive habit in rice. PLoS Genet **6**: e1000818

Whipple CJ, Zanis MJ, Kellogg EA, Schmidt RJ (2007) Conservation of B class gene expression in the second whorl of a basal grass and outgroups links the origin of lodicules and petals. Proc Natl Acad Sci USA **104**: 1081–1086

Wu D, Liang W, Zhu W, Chen M, Ferrándiz C, Burton RA, Dreni L, Zhang D (2018) Loss of LOFSEP transcription factor function converts spikelet to leaf-like structures in rice. Plant Physiol **176**: 1646–1664

Wu MF, Sang Y, Bezhani S, Yamaguchi N, Han SK, Li Z, Su Y, Slewinski TL, Wagner D (2012) SWI2/SNF2 chromatin remodeling ATPases overcome polycomb repression and control floral organ identity with the LEAFY and SEPALLATA3 transcription factors. Proc Natl Acad Sci USA **109**: 3576–3581

Xie M, Ren G, Zhang C, Yu B (2012a) The DNA- and RNA-binding protein FACTOR of DNA METHYLATION 1 requires XH domain-mediated complex formation for its function in RNA-directed DNA methylation. Plant J **72**: 491–500

Xie M, Ren G, Costa-Nunes P, Pontes O, Yu B (2012b) A subgroup of SGS3-like proteins act redundantly in RNA-directed DNA methylation. Nucleic Acids Res **40**: 4422–4431

Yan W, Chen D, Kaufmann K (2016) Molecular mechanisms of floral organ specification by MADS domain proteins. Curr Opin Plant Biol **29**: 154–162

Yuan Z, Gao S, Xue DW, Luo D, Li LT, Ding SY, Yao X, Wilson ZA, Qian Q, Zhang DB (2009) RETARDED PALEA1 controls palea development and floral zygomorphy in rice. Plant Physiol **149**: 235–244

Zahn LM, Kong H, Leebens-Mack JH, Kim S, Soltis PS, Landherr LL, Soltis DE, Depamphilis CW, Ma H (2005) The evolution of the *SEPALLATA* subfamily of MADS-box genes: a preangiosperm origin with multiple duplications throughout angiosperm history. Genetics **169**: 2209–2223

Zhang D, Wilson ZA (2009) Stamen specification and anther development in rice. Chin Sci Bull **54**: 1–12

Zhang D, Yuan Z (2014) Molecular control of grass inflorescence development. Annu Rev Plant Biol **65**: 553–578

Zhang CJ, Ning YQ, Zhang SW, Chen Q, Shao CR, Guo YW, Zhou JX, Li L, Chen S, He XJ (2012) IDN2 and its paralogs form a complex required for RNA-directed DNA methylation. PLoS Genet **8**: e1002693

Zhang D, Yuan Z, An G, Dreni L, Hu J, Kater MM (2013) Panicle development. Rice Genom Genet **5**: 279–295

Zhang J, Nallamilli BR, Mujahid H, Peng Z (2010) OsMADS6 plays an essential role in endosperm nutrient accumulation and is subject to epigenetic regulation in rice (*Oryza sativa*). Plant J **64**: 604–617

Zhang T, Li Y, Ma L, Sang X, Ling Y, Wang Y, Yu P, Zhuang H, Huang J, Wang N, (2017) *LATERAL FLORET 1* induced the three-florets spikelet in rice. Proc Natl Acad Sci USA **114**: 9984–9989

Zhang Y, Su J, Duan S, Ao Y, Dai J, Liu J, Wang P, Li Y, Liu B, Feng D, Wang J, Wang H (2011) A highly efficient rice green tissue protoplast system for transient gene expression and studying light/chloroplast-related processes. Plant Methods **7**: 30

Zheng Z, Xing Y, He XJ, Li W, Hu Y, Yadav SK, Oh J, Zhu JK (2010) An SGS3-like protein functions in RNA-directed DNA methylation and transcriptional gene silencing in *Arabidopsis*. Plant J **62**: 92–99

Zhu Y, Rowley MJ, Böhmdorfer G, Wierzbicki AT (2013) A SWI/SNF chromatin-remodeling complex acts in noncoding RNA-mediated transcriptional silencing. Mol Cell **49**: 298–309

Zuo J, Hare PD, Chua NH (2006) Applications of chemical-inducible expression systems in functional genomics and biotechnology. Methods Mol Biol **323**: 329–342